Printed on February 1, 2008

Electronic and Structural Properties of Carbon Nano-Horns

Savas Berber, Young-Kyun Kwon and David Tománek
Department of Physics and Astronomy, and Center for Fundamental Materials Research, Michigan State University, East Lansing, Michigan 48824-1116
(Received)

We use parametrized linear combination of atomic orbitals calculations to determine the stability, optimum geometry and electronic properties of nanometer-sized capped graphitic cones, called "nano-horns". Different nano-horn morphologies are considered, which differ in the relative location of the five terminating pentagons. Simulated scanning tunneling microscopy images of the various structures at different bias voltages reflect a net electron transfer towards the pentagon vertex sites. We find that the local density of states at the tip, observable by scanning tunneling spectroscopy, can be used to discriminate between different tip structures. Our molecular dynamics simulations indicate that disintegration of nano-horns at high temperatures starts in the highest-strain region near the tip.

61.48.+c, 61.50.Ah, 68.70.+w, 73.61.Wp

Since their first discovery[1], carbon nanotubes have drawn the attention of both scientists and engineers due to the large number of interesting new phenomena they exhibit[2–5], and due to their potential use in nanoscale devices: quantum wires[6], nonlinear electronic elements[7], transistors[8], molecular memory devices[9], and electron field emitters[10–13]. Even though nanotubes have not yet found commercially viable applications, projections indicate that this should occur in the very near future, with the advent of molecular electronics and further miniaturization of micro-electromechanical devices (MEMS). Among the most unique features of nanotubes are their electronic properties. It has been predicted that single-wall carbon nanotubes[14,15] can be either metallic or semiconducting, depending on their diameter and chirality[16–18]. Recently, the correlation between the chirality and conducting behavior of nanotubes has been confirmed by high resolution scanning tunneling microscopy (STM) studies[19,20].

Even though these studies have demonstrated that atomic resolution can be achieved[19–21], the precise determination of the *atomic configuration*, characterized by the chiral vector, diameter, distortion, and position of atomic defects, is still a very difficult task to achieve in nanotubes. Much of the difficulty arises from the fact that the electronic states at the Fermi level are only indirectly related to the atomic positions. Theoretical modeling of STM images has been found crucial to correctly interpret experimental data for graphite[22,23], and has been recently applied to carbon nanotubes[24,25]. As an alternative technique, scanning tunneling spectroscopy combined with modeling has been used to investigate the effect of the terminating cap on the electronic structure of nanotubes[26].

Among the more unusual systems that have been synthesized in the past few years are cone-shaped graphitic carbon structures[27,28]. Whereas similar structures have been observed previously near the end of multi-wall nanotubes[29], it is only recently that an unusually high production rate of up to 10 g/h has been achieved for single-walled cone-shaped structures, called "nano-horns", using the CO_2 laser ablation technique at room temperature in absence of a metal catalyst[30]. These conical nano-horns have the unique opening angle of $\approx 20°$.

We consider a microscopic understanding of the electronic and structural properties of nano-horns a crucial prerequisite for understanding the role of terminating caps in the physical behavior of contacts between nanotube-based nano-devices. So far, neither nano-horns nor other cone-shaped structures have been investigated theoretically. In the following, we study the structural stability of the various tip morphologies, and the interrelationship between the atomic arrangement and the electronic structure at the terminating cap, as well as the disintegration behavior of nano-horns at high temperatures.

Cones can be formed by cutting a wedge from planar graphite and connecting the exposed edges in a seamless manner. The opening angle of the wedge, called the disclination angle, is $n(\pi/3)$, with $0 \leq n \leq 6$. This disclination angle is related to the opening angle of the cone by $\theta = 2\sin^{-1}(1 - n/6)$. Two-dimensional planar structures (e.g. a graphene sheet) are associated with $n = 0$, and one-dimensional cylindrical structures, such as the nanotubes, are described by $n = 6$. All other possible graphitic cone structures with $0 < n < 6$ have been observed in a sample generated by pyrolysis of hydrocarbons[28]. According to Euler's rule, the terminating cap of a cone with the disclination angle $n(\pi/3)$ contains n pentagon(s) that substitute for the hexagonal rings of planar graphite.

The observed cone opening angle of $\approx 20°$, corresponding to a $5\pi/3$ disclination, implies that all nano-horns contain exactly five pentagons near the tip. We classify the structure of nano-horns by distinguishing the relative positions of the carbon pentagons at the apex which determine the morphology of the terminating cap. Our study will focus on the influence of the relative position

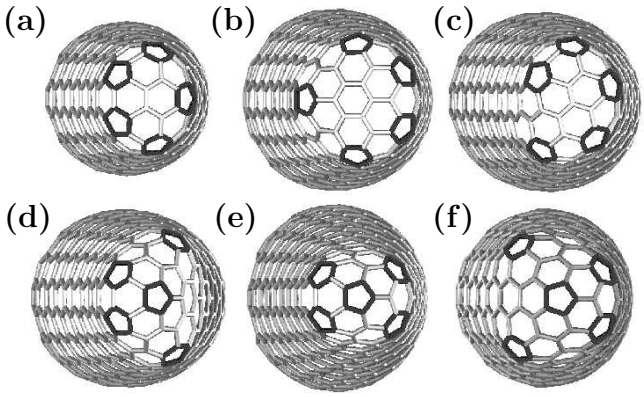

FIG. 1. Optimized carbon nano-horn structures with a total disclination angle of $5(\pi/3)$, containing five isolated pentagons at the terminating cap. Structures (a) – (c) contain all pentagons at the conical "shoulder", whereas structures (d) – (f) contain a pentagon at the apex. The pentagons are highlighted by a darker color.

of these five pentagons on the properties of nano-horns.

The cap morphologies investigated in this study are presented in Fig. 1. Nano-horns with all five pentagons at the "shoulder" of the cone, yielding a blunt tip, are shown in Figs. 1(a)–(c). Nano-horns with a pentagon at the apex of the tip, surrounded by the other four pentagons at the shoulder, are shown in Figs. 1(d)–(f). Note that the cone angle of each nano-horn is $\approx 20°$, even though the size of the terminating cap varies with the relative position of the pentagons.

To determine the structural and electronic properties of carbon nano-horns, we used the parametrized linear combination of atomic orbitals (LCAO) technique with parameters determined by *ab initio* calculations for simpler structures[31]. This approach has been found useful to describe minute electronic structure and total energy differences for systems with too large unit cells to handle accurately by *ab initio* techniques. Some of the problems tackled successfully by this technique are the electronic structure and superconducting properties of the doped C_{60} solid[32], the opening of pseudo-gaps near the Fermi level in a (10,10) nanotubes rope[33,34] and a (5,5)@(10,10) double-wall nanotube[35], as well as fractional quantum conductance in nanotubes[36]. This technique, combined with the recursion technique to achieve an $O(N)$ scaling, can determine very efficiently the forces on individual atoms[37], and had previously been used with success to describe the disintegration dynamics of fullerenes[38], the growth of multi-wall nanotubes[39] and the dynamics of a "bucky-shuttle"[9].

To investigate the structural stability and electronic properties of carbon nano-horns, we first optimized the structures with various cap morphologies, shown in Fig. 1. For the sake of an easier interpretation of our results, we distinguish the $N_{\rm cap} \approx 40 - 50$ atoms at the terminating cap from those within the cone-shaped mantle, that is terminated by $N_{\rm edge}$ atoms at the other end.

TABLE I. Structural data and stability results for carbon nano-horn structures (a)–(f), presented in Fig. 1. $N_{\rm tot} = N_{\rm tip} + N_{\rm edge}$ is the total number of atoms, which are subdivided into tip and edge atoms. $< E_{\rm coh,tot} >$ is the average binding energy, taken over the entire structure, and $< E_{\rm coh,tip} >$ the corresponding value excluding the edge region. $< E_{\rm coh,edge} >$ is the binding energy of the edge atoms, and $< E_{\rm coh,pent} >$ is the average over the pentagon sites in each system.

Quantity	(a)	(b)	(c)	(d)	(e)	(f)
$N_{\rm tot}$	205	272	296	290	308	217
$N_{\rm tip}$	172	233	257	251	270	180
$N_{\rm edge}$	33	39	39	39	38	37
$< E_{\rm coh,tot} >$ (eV)	−7.28	−7.29	−7.30	−7.30	−7.31	−7.28
$< E_{\rm coh,tip} >$ (eV)	−7.36	−7.36	−7.37	−7.36	−7.37	−7.36
$< E_{\rm coh,edge} >$ (eV)	−6.88	−6.88	−6.88	−6.88	−6.87	−6.89
$< E_{\rm coh,pent} >$ (eV)	−7.28	−7.28	−7.28	−7.28	−7.28	−7.28

We associate the tip region of a hypothetically infinite nano-horn with all the sites excluding the edge. Structural details and the results of our stability calculations are presented in Table I. These results indicate that atoms in nano-horns are only ≈0.1 eV less stable than in graphite. The relative differences in $< E_{\rm coh,tot} >$ reflect the strain energy changes induced by the different pentagon arrangements. To minimize the effect of under-coordinated atoms at the edge on the relative stabilities, we excluded the edge atoms from the average when calculating $< E_{\rm coh,tip} >$. Since our results for $< E_{\rm coh,tip} >$ and $< E_{\rm coh,tot} >$ follow the same trends, we believe that the effect of edge atoms on the physical properties can be neglected for structures containing hundreds of atoms. Even though the energy differences may appear minute on a per-atom basis, they translate into few electron-volts when related to the entire structure. Our results suggest that the under-coordinated edge atoms are all less stable than the cone mantle atoms by ≈0.5 eV. Also atoms in pentagons are less stable than those in hexagons by ≈0.1 eV, resulting in an energy penalty of ≈0.5 eV to create a pentagon if the strain energy induced by bending the lattice could be ignored.

When comparing the stabilities of the tip regions, described by $< E_{\rm coh,tip} >$, we found no large difference between blunt tips that have all the pentagons distributed along the cylinder mantle and pointed tips containing a pentagon at the apex. We found the structure shown in Fig. 1(c) to be more stable than the other blunt structures with no pentagon at the apex. Similarly, the structure shown in Fig. 1(e) is most stable among the pointed tips containing a pentagon at the apex. Equilibrium carbon-carbon bond lengths in the cap region are $d_{CC} = 1.43 - 1.44$ Å at the pentagonal sites and $d_{CC} = 1.39$ Å at the hexagonal sites, as compared to $d_{CC} = 1.41 - 1.42$ Å in the mantle. This implies that the "single bonds" found in pentagons should be weaker than the "double bonds" connecting hexagonal sites, thus con-

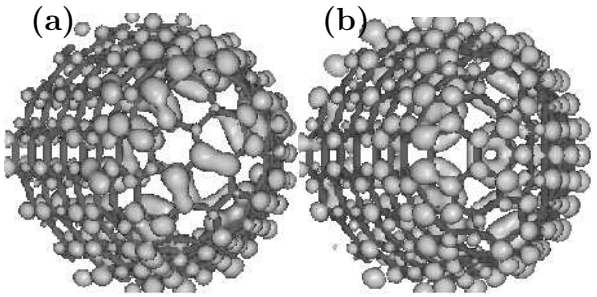

FIG. 2. Simulated STM images in the tip region for (a) the nano-horn shown in Fig. 1(c) and (b) the nano-horn shown in Fig. 1(d). These results for the occupied electronic states near the Fermi level, corresponding to the bias voltage of $V_b = 0.2$ V, are suggestive of a net electron transfer from the hexagonal to the pentagonal sites. The charge density contour displayed corresponds to the value of $\rho = 1.35\times10^{-3}$ electrons/Å^3. Dark lines depict the atomic bonds to guide the eye.

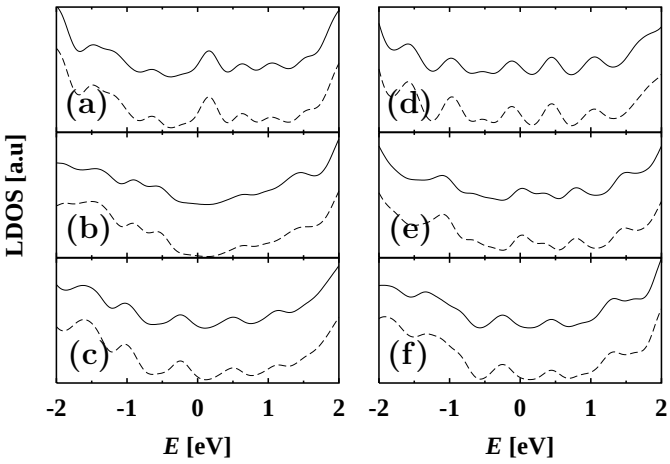

FIG. 3. Local electronic densities of states, normalized per atom and shown in consistent arbitrary units, for the terminating cap of the tip (solid line) and for the pentagon sites only (dashed line) of nano-horn structures shown in Fig. 1. The similarity between the results for the entire cap and the pentagon sites necessitated a vertical offset of one set of data for an easy distinction, thus indicating that variations in the arrangement of pentagons affect the densities of states not only at the pentagonal sites, but within the entire cap region. The most marked differences are noted near the Fermi level, at $E\approx0$ eV.

firming our results in Table I and the analogous behavior in the C_{60} molecule.

Since pentagon sites are defects in an all-hexagon structure, they may carry a net charge. To characterize the nature of the defect states associated with these sites, we calculated the electronic structure at the tip of the nano-horns. The charge density associated with states near E_F, corresponding to the local density of states at that particular position and energy, is proportional to the current observed in STM experiments. To compute the local charge density associated with a given eigenstate, we projected this state onto a local atomic basis. The projection coefficients were used in conjunction with real-space atomic wave functions from density functional calculations[23] to determine the charge density corresponding to a particular level or the total charge density. To mimic a large structure, we convoluted the discrete level spectrum by a Gaussian with a full-width at half-maximum of 0.3 eV. Using this convoluted spectrum, we also determined the charge density associated with particular energy intervals corresponding to STM data for a given bias voltage.

In Fig. 2, we present such simulated STM images for the nano-horns represented in Figs. 1(c) and 1(d). We show the charge density associated with occupied states within a narrow energy interval of 0.2 eV below the Fermi level[40] as three-dimensional charge density contours, for the density value of $\rho = 1.35 \times 10^{-3}$ electrons/Å^3. Very similar results to those presented in Fig. 2 were obtained at a higher bias voltage of 0.4 eV. As seen in Fig. 2, $pp\pi$ interactions dominate the spectrum near E_F. These images also show a net excess charge on the pentagonal sites as compared to the hexagonal sites. This extra negative charge at the apex should make pointed nano-horn structures with a pentagon at the apex better candidates for field emitters[10–13] than structures with no pentagon at the apex and a relatively blunt tip.

It has been shown previously that theoretical modeling of STM images is essential for the correct interpretation of experimental data. Atomically resolved STM images, however, are very hard to obtain especially near the terminating caps of tubes[26] and cones, due to the large surface curvature that can not be probed efficiently using current cone-shaped STM tips. A better way to identify the tip structure may consist of scanning tunneling spectroscopy (STS) measurements in the vicinity of the tip. This approach is based on the fact that in STS experiments, the normalized conductance $(V/I)(dI/dV)$ is proportional to the local density of states which, in turn, is structure sensitive. We have calculated the local density of states at the terminating cap of the tips for the different nano-horn structures shown in Fig. 1. Our results are shown in Fig. 3, convoluted using a Gaussian with a full-width at half-maximum of 0.3 eV.

To investigate the effect of pentagonal sites on the electronic structure at the tip, we first calculated the local density of states only at the 25 atoms contained in the five terminating pentagons. The corresponding densities of states, shown by the dashed curve in Fig. 3, are found to vary significantly from structure to structure near the Fermi level[40]. Thus, a comparison between the densities of states at $E\approx E_F$ should offer a new way to discriminate between the various tip morphologies. For an easy comparison with experiments, we also calculated the local density of states in the entire terminating cap, including all five pentagons and consisting of $N\approx40-50$ atoms,

depending on the structure. The corresponding density of states, given by the solid line in Fig. 3, is vertically displaced for easier comparison. Our results show that the densities of states, both normalized per atom, are very similar. Thus, we conclude that the pentagonal sites determine all essential features of the electronic structure near the Fermi level at the tip.

Next, we have studied the heat resilience[30] as well as the decay mechanism of nano-horns at extremely high temperatures using molecular dynamics simulations[41]. In our canonical molecular dynamics simulations, we keep the structure at a constant temperature using a Nosé-Hoover thermostat[42], and use a fifth–order Runge–Kutta interpolation scheme to integrate the equations of motion, with a time step of $\Delta t = 5 \times 10^{-16}$ s. We found the system to remain structurally intact within the temperature range from $T = 2,000 - 4,000$ K. Then, we heated up the system gradually from $T = 4,000$ K to $5,000$ K within 4,000 time steps, corresponding to a time interval of 2 ps. Our molecular simulations show that nano-horn structures are extremely heat resilient up to $T \lesssim 4,500$ K. At higher temperatures, we find these structures to disintegrate preferentially in the vicinity of the pentagon sites. A simultaneous disintegration of the nano-horn structures at the exposed edge, which also occurs in our simulations, is ignored as an artifact of finite-size systems. The preferential disintegration in the higher strain region near the pentagon sites, associated with a large local curvature, is one reason for the observation that nano-horn tips are opened easily at high temperatures, in presence of oxygen[30].

In summary, we used parametrized linear combination of atomic orbitals calculations to determine the stability, optimum geometry and electronic properties of nanometer-sized capped graphitic cones, called nano-horns. We considered different nano-horn morphologies that differ in the relative location of the five terminating pentagons. We found a net electron transfer to the pentagonal sites of the cap. This extra charge is seen in simulated scanning tunneling microscopy images of the various structures at different bias voltages. We found that the local density of states at the tip, observable by scanning tunneling spectroscopy, can be used to discriminate between different tip structures. Our molecular dynamics simulations indicate that disintegration of nano-horns at high temperatures starts in the highest-strain region near the tip.

We thank S. Iijima for fruitful discussions on carbon nano-horns. We acknowledge financial support by the Office of Naval Research and DARPA under Grant Number N00014-99-1-0252.

[1] Sumio Iijima, Nature **354**, 56 (1991).

[2] M.S. Dresselhaus, G. Dresselhaus, and P.C. Eklund, *Science of Fullerenes and Carbon Nanotubes* (Academic Press, 1996, San Diego).

[3] T.W. Ebbesen, Phys. Today **49** (6), 26 (1996).

[4] B.I. Yakobson and R.E. Smalley, Am. Sci. **85**, 324 (1997).

[5] R. Saito, G. Dresselhaus, and M.S. Dresselhaus, *Physical Properties of Carbon Nanotubes* (Imperial College Press, 1998).

[6] S.J. Tans, Michel H. Devoret, Hongjie Dai, Andreas Thess, Richard E. Smalley, L.J. Geerligs, and Cees Dekker, Nature **386**, 474 (1997)

[7] M. Bockrath, David H. Cobden, Paul L. McEuen, Nasreen G. Chopra, A. Zettl, Andreas Thess, and R.E. Smalley, Science **275**, 1922 (1997).

[8] S.J. Tans, A.R.M. Verschueren, and C. Dekker, Nature **393**, 49 (1998).

[9] Young-Kyun Kwon, David Tománek, and Sumio Iijima, Phys. Rev. Lett. **82**, 1470 (1999).

[10] A.G. Rinzler, J.H. Hafner, P. Nikolaev, L. Lou, S.G. Kim, D. Tománek, P. Nordlander, D.T. Colbert, and R.E. Smalley, Science **269**, 1550 (1995).

[11] W.A. de Heer, A. Châtelain, and D. Ugarte, Science **270**, 1179 (1995).

[12] L.A. Chernozatonskii, Y.V. Gulyaev, Z.J. Kosakovskaja, N.I. Sinitsyn, G.V. Torgashov, Y.F. Zakharchenko, E.A. Fedorov, and V.P. Valchuk, Chem. Phys. Lett. **233**, 63 (1995).

[13] W.B. Choi, D.S. Chung, J.H. Kang, H.Y. Kim, Y.W. Jin, I.T. Han, Y.H. Lee, J.E. Jung, N.S. Lee, G.S. Park, J.M. Kim, Appl. Phys. Lett. **75**, 3129 (1999).

[14] S. Iijima and T. Ichihashi, Nature **363**, 603 (1993).

[15] D.S. Bethune, C.H. Kiang, M.S. de Vries, G. Gorman, R. Savoy, J. Vazquez, R. Beyers, Nature **363**, 605 (1993).

[16] J.W. Mintmire, B.I. Dunlap, and C.T. White, Phys. Rev. Lett. **68**, 631 (1992).

[17] R. Saito, M. Fujita, G. Dresselhaus, and M.S. Dresselhaus, Appl. Phys. Lett. **60**, 2204 (1992).

[18] N. Hamada, S. Sawada, and A. Oshiyama, Phys. Rev. Lett. **68**, 1579 (1992).

[19] J.W.G. Wildöer, L.C. Venema, A.G. Rinzler, R.E. Smalley, and C. Dekker, Nature **391**, 59 (1998).

[20] T.W. Odom, J.-L. Huang, P. Kim, and C.M. Lieber, Nature **391**, 62 (1998).

[21] W. Clauss, D.J. Bergeron, and A.T. Johnson Phys. Rev. B **58**, R4266 (1998).

[22] David Tománek, Steven G. Louie, H. Jonathon Mamin, David W. Abraham, Ruth Ellen Thomson, Eric Ganz, and John Clarke, Phys. Rev. B **35**, 7790 (1987);

[23] David Tománek and Steven G. Louie, Phys. Rev. B **37**, 8237 (1988).

[24] V. Meunier, Ph. Lambin, Phys. Rev. Lett. **81**, 5588 (1998).

[25] C.L. Kane and E.J. Mele, Phys. Rev. B **59**, R12759 (1999).

[26] Philip Kim, Teri W. Odom, Jin-Lin Huang, and Charles M. Lieber, Phys. Rev. Lett. **82**, 1225 (1999).

[27] M. Ge, and K. Sattler, Chem. Phys. Lett. **220**, 192 (1994).

[28] A. Krishnan, E. Dujardin, M.M.J. Treacy, J. Hugdahl, S. Lynum, and T.W. Ebbesen, Nature **388**, 451 (1997).

[29] S. Iijima, T. Ichihashi, and Y. Ando, Nature **356**, 776 (1992).

[30] S. Iijima, M. Yudasaka, R. Yamada, S. Bandow, K. Sue-

naga, F. Kokai, and K. Takahashi, Chem. Phys. Lett. **309**, 165 (1999).
[31] D. Tománek and Michael A. Schluter, Phys. Rev. Lett. **67**, 2331 (1991).
[32] M. Schluter, M. Lannoo, M. Needels, G.A. Baraff, and D. Tománek, Phys. Rev. Lett. **68**, 526 (1992).
[33] Young-Kyun Kwon, Susumu Saito, and David Tománek Phys. Rev. B **58**, R13314 (1998).
[34] Young-Kyun Kwon, David Tománek, Young Hee Lee, Kee Hag Lee, and Susumu Saito, J. Mater. Res. **13** 2363 (1998).
[35] Young-Kyun Kwon and David Tománek, Phys. Rev. B **58**, R16001 (1998).
[36] Stefano Sanvito, Young-Kyun Kwon, David Tománek, and Colin J. Lambert, Phys. Rev. Lett. **84**, 1974 (2000).
[37] W. Zhong, D. Tománek, and G.F. Bertsch, Solid State Commun. **86**, 607 (1993).
[38] S.G. Kim and D. Tománek, Phys. Rev. Lett. **72**, 2418 (1994).
[39] Young-Kyun Kwon, Young Hee Lee, Seong Gon Kim, Philippe Jund, David Tománek, and Richard E. Smalley, Phys. Rev. Lett. **79**, 2065 (1997).
[40] The nano-horn structures considered in our calculation are clusters containing edge atoms. We found that due to the charge transfer towards the under-coordinated atoms at the edge, the "Fermi level" of these clusters may drop by as much as $\approx 1.0 - 1.2$ eV with respect to that of a graphene monolayer. To compensate for this artifact, we excluded the edge region from the calculated density of states and found the E_F value to lie very close to that of a graphene monolayer.
[41] M.P. Allen and D.J. Tildesley, *Computer Simulation of Liquids* (Clarendon Press, 1987 Oxford).
[42] S. Nosé, Mol. Phys. **52**, 255 (1984); W.G. Hoover, Phys. Rev. A **31**, 1695 (1985).